

# Chaotic transitions of optomechanical resonator modified by the quadratic coupling

L. Zhang and X. Zhang

*School of physics and Information Technology, Shaanxi Normal University, Xi'an 710061, China*

W. P. Zhang

*Department of Physics, East China Normal University, Shanghai 200062, China*

A parametric modification of the dynamical transition from steady-state to limit circles and to chaos by the quadratic coupling in optomechanical system is investigated. Under a weak pumping field, the mechanical resonator damps to a steady state with a controllable nonlinear property, and then, when the driving power reaches a critical threshold, the steady state loses its stability and locks on a limit-circle oscillation (self-oscillation) with an increasing and jumping amplitude. Along with an increase of the driving power, the period-doubling bifurcations to chaos followed by the inversion bifurcations back to limit circles are found and verified by the numerical calculation of their maximal Lyapunov Exponents. Our study shows that the structure of bifurcation and inverse bifurcation can be easily modified by a weak shift of quadratic coupling, and the dynamical transitions between self-oscillation and chaos can easily be traced or detected by the power spectrum of the cavity field.

PACS numbers: 42.50.Wk, 05.45.-a, 07.10.Cm, 42.50.Ct

## I. INTRODUCTION

In recent years, continuing interest on cavity optomechanical systems stimulates the study of light driven nanomechanical oscillator to develop light-controlled ultrasensitive force and mass sensors or field-driven signal processors [1, 2]. In a weak driving regime, the quantum behaviors of the mechanical oscillator are mainly focused on, such as cooling the mechanical oscillator into a quantum ground state by red-detuned pumping field in order to control or engineer its quantum evolution [3, 4]. Otherwise, especially in a strong, blue-detuned pumping field, a large displacement of the mechanical oscillator can intrigue manifest nonlinear effect of the system and the nonlinear classical dynamics beyond quantum behavior becomes more interesting to explore new features of classical nonlinear dynamics [5–8]. One important classical behavior found in the optomechanical systems is that the system can establish a stable self-sustained oscillation (SSO) [9–13]. An easily controlled SSO is a basic precondition for a physical application of developing signal sensors or processors based on nanomechanical systems [14]. A conventional optomechanical system only considers the linear photon-phonon coupling, whose magnitude is linearly proportional to the displacement of the mechanical resonator, because the displacement of the mechanical oscillator is very small and the quadratic coupling is very weak. Recently, Bakemeier et. al. [15] found a very interesting chaotic dynamics in the linear coupling optomechanical system and closely studied its typical routes to chaos in a blue-detuned pumping case. They clearly demonstrated a sequence of period-doubling bifurcations leading to chaos in a conventional optomechanical system. However, for a large displacement under a strong field pumping, the weak nonlinear quadratic coupling will be critical to a nonlinear dynamics and the nonlinear photon-phonon coupling properties of the system

should be included [16]. As shown in many optomechanical systems [16–22], the nonlinear couplings play important roles even in a weak red-detuned pumping system and can lead to more interesting nonlinear effects than what we expected in a variety of optomechanical systems [23–28].

Therefore, in this paper, we mainly consider the classical dynamic transitions of the optomechanical resonator modified by the quadratic couplings combined with the linear coupling and find a rich chaotic behavior of the optomechanical resonator beyond a blue-detuned pumping field. The combination of linear and quadratic coupling provides a tunable nonlinearity for the light field and for the mechanical resonator, and which can be exploited for the sensitive on-chip signal processor and sensor enhanced by nonlinear effects [26]. The dynamical transition behaviors on this model will give a basic physical approach to modify the mechanical dynamics through the quadratic coupling rate of the system, especially in a critical region where the nonlinear property has an enhanced sensitivity to the external signals.

## II. THE MODEL

The Hamiltonian of a one-dimensional optomechanical system with both linear and quadratic couplings can be written as [1, 13]

$$\hat{H} = \hat{H}_M + \hat{H}_{\text{opt}} + \hat{H}_{\text{pump}} + \hat{H}_\kappa + \hat{H}_\gamma, \quad (1)$$

where

$$\begin{aligned} \hat{H}_M &= \frac{\hat{p}^2}{2M} + \frac{1}{2}M\omega_M^2\hat{x}^2, \\ \hat{H}_{\text{opt}} &= -\hbar\delta_c\hat{a}^\dagger\hat{a} + \hbar g_1\hat{a}^\dagger\hat{a}\hat{x} + \frac{1}{2}\hbar g_2\hat{a}^\dagger\hat{a}\hat{x}^2 \\ \hat{H}_{\text{pump}} &= i\hbar[\eta(t)\hat{a}^\dagger - \eta^*(t)\hat{a}]. \end{aligned}$$

In above model, the mechanical resonator  $\hat{H}_M$  with a free frequency of  $\omega_M$  interacts with a cavity mode  $\hat{H}_{\text{opt}}$  of frequency  $\omega_c$  through the linear pressure coupling rate of  $g_1$  and the dispersive quadratic coupling rate of  $g_2$ . The quadratic coupling can be effectively derived not only from the nonlinear deformation of the cavity field but also from the nonlinear properties of the mechanical resonators [12, 29, 30].  $\hat{H}_{\text{pump}}$  describes the cavity pumping with a frequency of  $\omega_p$  and an amplitude of  $\eta$  related to the driving power  $P$  by  $|\eta|^2 = P\kappa/\hbar\omega_p$ .  $\hat{H}_\kappa$  and  $\hat{H}_\gamma$  are the baths coupled to the cavity mode and the mechanical resonator and induce energy dissipations with the damping rates of  $\kappa$  and  $\gamma_M$ , respectively. In above model, the pump-cavity detuning is defined by  $\delta_c = \omega_p - \omega_c$ , and  $g_1, g_2$  are given by  $g_1 = \omega'_c(x)$ ,  $g_2 = \omega''_c(x)$  for a linear cavity, where the prime means the spatial derivative [1]. For example, in a linear Fabry-Porot (FP) cavity, the cavity mode of  $\omega_c(x)$  can give  $g_1 = -\omega_0/L_0$  and  $g_2 = 2\omega_0/L_0^2$ , respectively.

Based on the cross-coupling Hamiltonian (1), the Heisenberg equation of motion for the mechanical resonator reads

$$\frac{d^2\hat{x}}{dt^2} + \frac{\gamma_M}{2} \frac{d\hat{x}}{dt} + \omega_M^2 \left( 1 + \frac{\hbar g_2}{M\omega_M^2} \hat{a}^\dagger \hat{a} \right) \hat{x} = -\frac{\hbar g_1}{M} \hat{a}^\dagger \hat{a} + \frac{\hat{\xi}(t)}{M},$$

where  $\hat{\xi}(t)$  accounts for the Langevin noise of the mechanical resonator. Above equation indicates that the quadratic coupling leads to a direct frequency modification of the mechanical resonator via the cavity field intensity of  $\hat{a}^\dagger \hat{a}$ . Although the quadratic coupling is very weak, its parametric effect on the mechanical oscillator becomes manifest if the intensity of the cavity field becomes strong. The intensity of the cavity mode is determined by

$$\frac{d}{dt} \hat{a}^\dagger \hat{a} = \eta \hat{a}^\dagger + \eta^* \hat{a} - \kappa \hat{a}^\dagger \hat{a} + \sqrt{\kappa} \left( \hat{a}^\dagger \hat{a}_{in} + \hat{a}_{in}^\dagger \hat{a} \right),$$

where  $\hat{a}_{in}$  is the input noise of the light mode. Therefore, according to above dynamical equations, the optomechanical system with both linear and quadratic couplings results in a field-driven parametric oscillator [31–33] with a modulated frequency of  $\omega_M \sqrt{1 + \hbar g_2 \hat{a}^\dagger \hat{a} / (M\omega_M^2)}$ .

As in the case of a large displacement of the mechanical oscillator in a strong pumping field, the classical dynamics above all quantum fluctuations is dominated. The classical dynamics of this cavity-resonator system is investigated by replacing all the quantum operators with their corresponding complex  $c$  numbers, such as  $\hat{x} \rightarrow \langle \hat{x} \rangle = x_c, \hat{p} \rightarrow \langle \hat{p} \rangle = p_c, \hat{a} \rightarrow \langle \hat{a} \rangle = a_c$  without considering any quantum fluctuations and correlations [34]. Then the classical dynamics of the system is governed by

the following system of equations:

$$\begin{aligned} \frac{dx(\tau)}{d\tau} &= p(\tau), \\ \frac{dp(\tau)}{d\tau} &= -\frac{\gamma_M}{2} p - \Omega^2(\tau) x(\tau) - 2\omega_1 I(\tau) \\ \frac{dX(\tau)}{d\tau} &= -[\delta_c - \omega_1 x(\tau) - \omega_2 x^2(\tau)] Y(\tau) \\ &\quad - \frac{\kappa}{2} X(\tau) + \eta(\tau), \\ \frac{dY(\tau)}{d\tau} &= [\delta_c - \omega_1 x(\tau) - \omega_2 x^2(\tau)] X(\tau) - \frac{\kappa}{2} Y(\tau), \end{aligned} \quad (2)$$

where  $x(\tau) = x_c/x_{\text{zpf}}$  and  $p(\tau) = p_c/p_{\text{zpf}}$  are the position and the momentum of the mechanical resonator scaled by  $x_{\text{zpf}} = \sqrt{\hbar/2M\omega_M}$  and  $p_{\text{zpf}} = \sqrt{\hbar M\omega_M/2}$ , repetitively. The two field quadratures  $X(\tau)$  and  $Y(\tau)$  are defined by  $X(\tau) = (a_c + a_c^*)/2$  and  $Y(\tau) = -i(a_c - a_c^*)/2$  with the field intensity being  $I(\tau) = X^2(\tau) + Y^2(\tau)$ . Then the classical dynamic equation of the mechanical resonator is

$$\ddot{x}(\tau) + \frac{\gamma_M}{2} \dot{x}(\tau) + \Omega^2(\tau) x(\tau) = -2\omega_1 I(\tau), \quad (3)$$

where the field modulated frequency of the mechanical resonator  $\Omega(\tau) = \sqrt{1 + 4\omega_2 I(\tau)}$ . Particularly, the scaled linear and quadratic coupling frequencies are

$$\omega_1 = g_1 x_{\text{zpf}}/\omega_M, \omega_2 = \frac{1}{2} g_2 x_{\text{zpf}}^2/\omega_M, \quad (4)$$

respectively, and all the other parameters  $\delta_c, \gamma_M, \kappa$  are scaled by  $\omega_M$  (use the same labels for convenient) with a scaled time  $\tau = \omega_M t$ . In above equations, the dynamical influences of the equilibrium baths  $\hat{H}_\kappa$  and  $\hat{H}_\gamma$  are supposed to be zero for  $\langle a_{in}(\tau) \rangle = 0, \langle \xi(\tau) \rangle = 0$  and the classical pumping field is supposed to be a real function of  $\eta(\tau)$  scaled by  $\omega_M$ . All the parameters used in the following calculations are from the relevant experimental results and analyzed in detail in Ref.[13, 18]. As Eq.(2) totally describes a parametric oscillator with a field-modulated frequency through the quadratic optomechanical coupling, a modification of quadratic coupling can surely change the dynamics of the mechanical oscillator in a strong pumping field.

### III. STEADY-STATE PROPERTIES

In a weak pumping field, the optomechanical resonator will settle down to a steady state due to the energy damping. The static response of the resonator is then determined by [35]

$$x_s = -\frac{2\omega_1 I_s}{1 + 4\omega_2 I_s}, \quad (5)$$

$$I_s = \frac{|\eta|^2}{(\kappa/2)^2 + (\delta_c - \omega_1 x_s - \omega_2 x_s^2)^2}, \quad (6)$$

where  $I_s \equiv X_s^2 + Y_s^2$  is the steady intensity of the cavity field and  $|\eta|^2$  is the scaled input pumping power.

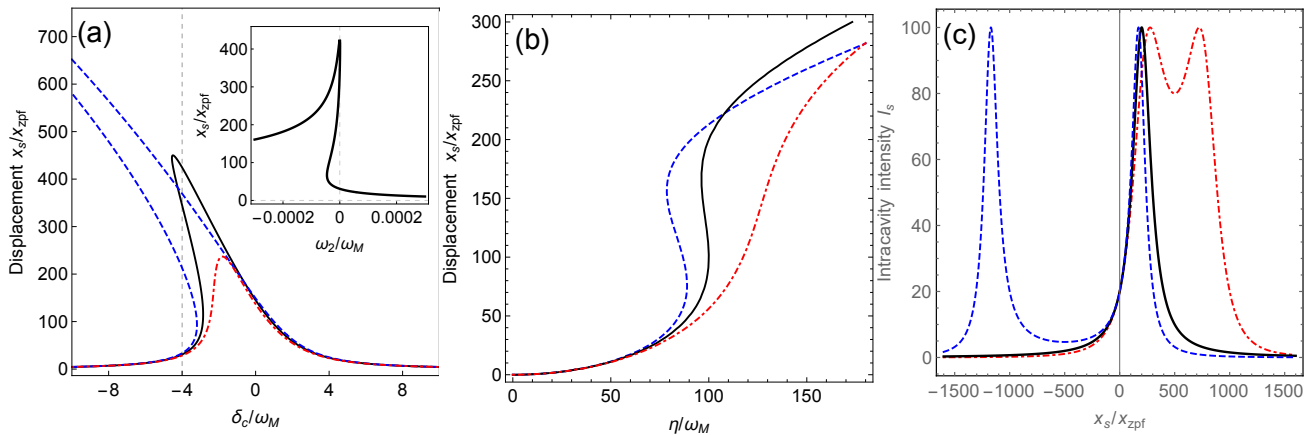


FIG. 1: (a) Static displacement  $x_s$  versus pump detuning  $\delta_c$  with a fixed pumping amplitude  $\eta = 150$ . Inset:  $x_s$  changes with the quadratic coupling under  $\delta_c = -4, \eta = 150$ . (b) The bistability response of  $x_s$  to the pumping amplitude  $\eta$  with a fixed detuning of  $\delta_c = -2$ . (c) The intracavity intensity  $I_s$  varies with  $x_s$  under  $\eta = 10, \delta_c = -2$ . The linear coupling  $\omega_1 = -0.01$ , the quadratic couplings are  $\omega_2 = -10^{-5}$  (blue dashed lines),  $\omega_2 = 0$  (black solid lines),  $\omega_2 = 10^{-5}$  (red dot and dashed lines), respectively, and the cavity damping rate  $\kappa = 2$ .

Above solutions demonstrate a clear nonlinear response of the mechanical resonator to the light field in a red-detuned pumping region ( $\delta_c < 0$ ) [36, 37]. As shown in Fig.1(a)(b), the static displacement of the resonator is sensitive to a modification of quadratic coupling in the strong pumping regime [12]. Fig.1(a)(b) reveals that a negative quadratic coupling can enhance the nonlinear property of the mechanical resonator, and Fig.1(c) demonstrates a double resonant peak of the intracavity intensity to the resonator's position. The splitting of the normal Lorentzian line shape of the cavity intensity (solid line in Fig.1(c)) is a characteristic property of the quadratic coupling in optomechanical system and which can be used to detect the quadratic coupling rate by measuring the splitting of  $\sqrt{\omega_1^2 + 4\delta_c\omega_2/\omega_2}$  provided the linear coupling  $\omega_1$  is known.

According to Eq.(5), the static displacement of the resonator approximately increases with the intensity of the cavity field, i.e.  $\propto -\omega_1 I_s$ , and the parametric modification of the quadratic coupling is based on the linear coupling  $\omega_1$ . Although in most cases the quadratic coupling  $\omega_2$  is much smaller than the linear coupling  $\omega_1$ , it can still bring dramatic effects on the mechanical resonator if it meets a resonant case of  $\omega_2 \sim -1/(4I_s)$  (see the inset of Fig.1(a)). Above static responses modified by quadratic couplings can be completely understood by the adiabatic potential generated by the cavity mode because the field modulation is much faster than that of the mechanical resonator. The total adiabatic potential felt by the mechanical resonator is [13]

$$U(x, \tau) = \frac{1}{2}x^2 - \frac{4\eta^2(\tau)}{\kappa} \arctan\left[\frac{\Delta(x)}{\kappa/2}\right], \quad (7)$$

where the effective position dependent detuning  $\Delta(x) = \delta_c - \omega_1 x - \omega_2 x^2$ . This light-dressed adiabatic potential is a sum of harmonic potential and a field-induced potential

of arctangent function. In a large pumping amplitude  $\eta$ , the field-induced potential,  $-\frac{4\eta^2}{\kappa} \arctan\left[\frac{\Delta(x)}{\kappa/2}\right]$ , greatly influences the harmonic part by introducing more equilibria to the harmonic potential. As the nonlinear response of the resonator is manifest in a red-detuned pumping region ( $\delta_c < 0$ ) shown in Fig.1, in the following sections, we will focus on the nonlinear dynamics of the mechanical resonator with both linear and quadratic couplings mainly in a red-detuned region.

#### IV. CHAOTIC TRANSITIONS

Certainly, above nonlinear steady-state behaviors are based on the steady solutions of the system without considering their dynamical stabilities and, thus, most of the static behaviors are actually fake because the system never goes to a steady state of Eq.(5) and Eq.(6) when the pumping field is above a threshold power [11–13]. The dynamical behavior deviates from a steady-state response of Eq.(5) (the dashed line) is shown in Fig.2 by a jumping and bifurcation process. As the system is not a conservative system without time reversibility [38], we only consider the dynamics starting with a zero initial conditions from a control point of view.

When the input energy from the pumping field exceeds the dissipative energy of field and resonator, the steady state will burst into a self-oscillation through a Hopf bifurcation process [39] and then transit to a chaotic oscillation via a typical period-doubling bifurcation route [6, 15]. A complete responsive dynamics of a light-driven mechanical resonator are shown in Fig.2 and which demonstrates three different dynamical transitions from steady state to self-oscillation, then to chaotic dynamics and finally back to self-oscillation again as the pumping power is continuously increased. The inset of Fig.2 dis-

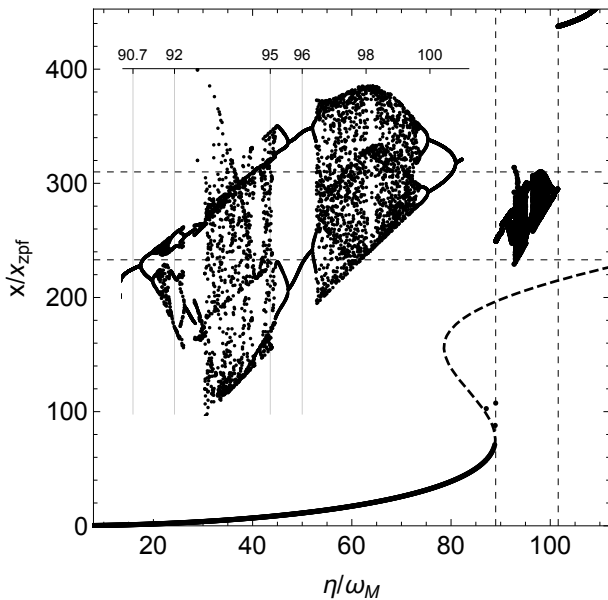


FIG. 2: The typical bifurcation of mechanical resonator's positive position versus the pumping amplitude  $\eta$ . The parameters are  $\kappa = 2, \gamma_M = 0.01, \delta_c = -2, \omega_1 = -0.01$  and  $\omega_2 = -10^{-5}$  with the zero initial conditions of  $x(0) = p(0) = X(0) = Y(0) = 0$ . The dashed line is the steady-state response. The inset shows the zoomed-in bifurcation from the dashed rectangle.

plays the details of the period-doubling route to chaos and the inverse bifurcation route back to self-oscillation along with an increasing pumping power. We find a rich structure of the bifurcation and the inverse bifurcation windows [5] embedded in the pumping region from  $\eta = 90$  to  $\eta = 101$  under the parameters shown in Fig.2.

Fig.3 picks several typical dynamical orbits of the optomechanical resonator in the phase space at specific pumping powers to demonstrate one window of period-doubling bifurcation to inverse bifurcation. At  $\eta = 90.7$  shown in Fig.3(a), the resonator takes an attractive period-1 orbit (a stable limit circle) and then breaks into a period-4 orbit at  $\eta = 92$  shown in Fig.3(b). One of chaotic attractor is formed at  $\eta = 95$  shown in Fig.3(c) and then returns back to a 2-period orbit when the pumping amplitude increases to  $\eta = 96$  via an inverse bifurcation process.

We can verify this interesting chaotic dynamics by calculating the maximal Lyapunov exponent (MLE) of the system as shown in Fig.4. The MLE can discriminate three different dynamics of the resonator, the steady-state behavior with a negative MLE, the limit-circle dynamics with a zero MLE, and a clear positive MLE in the chaotic window with abrupt droppings near to zero (inset of Fig.4). The very interesting thing is that the stability of the system is enhanced by a clear dropping of MLE at the critical pumping threshold around  $\eta = 89$ . This effect is due to the static "spring" effect of the light field [40, 41] which is proportional to  $\eta^2$  (see Eq.(7)) and

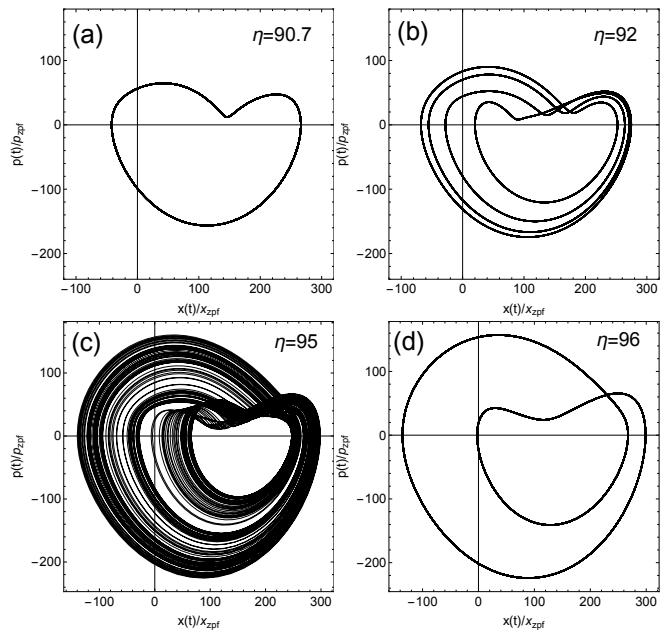


FIG. 3: The samples of the dynamical orbits of mechanical oscillation in the phase space for the bifurcation points at (a)  $\eta = 90.7$ , (b)  $\eta = 92$ , (c)  $\eta = 95$ , and (d)  $\eta = 96$ . The other parameters are the same as that in Fig.2.

can also be modified by the quadratic coupling. The zero value of MLE beyond the chaotic windows is a clear signature of the limit-circle dynamics of the resonator. For a motion on a limit circle, the LE perpendicular to the orbit is negative but it is zero along the trajectory indicating a phase freedom of the motion. This phase freedom is the well-known mechanism leading to synchronization of a collection of resonators on the limit circle because

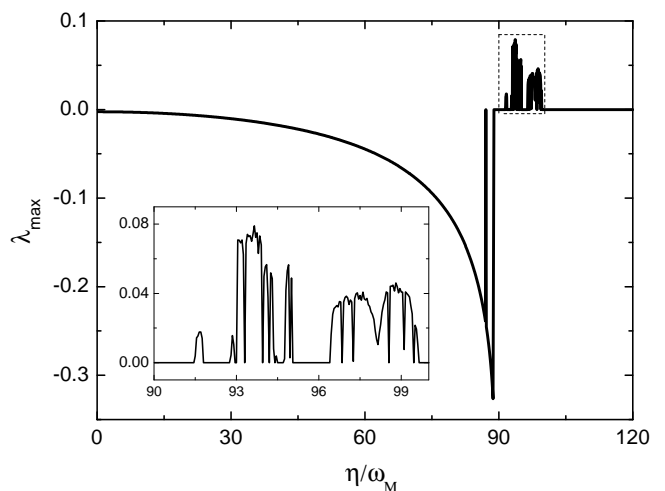


FIG. 4: The maximum Lyapunov exponent of the optomechanical oscillator corresponding to Fig.2. The inset shows the zoomed image from the dashed rectangle. The parameters are the same as that shown in Fig.2.

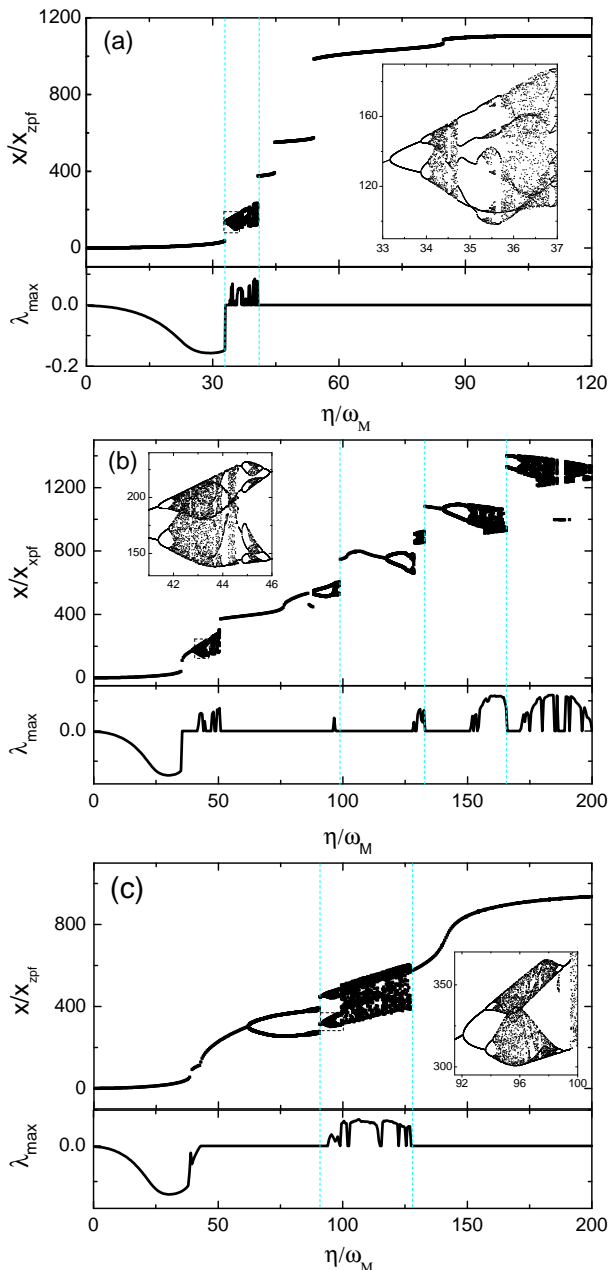


FIG. 5: Displacement bifurcations (top) and the corresponding maximal Lyapunov exponents (bottom) of the mechanical resonator vs pumping amplitude  $\eta$  modified by the quadratic couplings of (a)  $\omega_2 = -10^{-5}$ , (b)  $\omega_2 = 0$ , and (c)  $\omega_2 = 10^{-5}$ . The insets show the zoomed-in bifurcation images from the corresponding dashed rectangles. The other parameters are  $\omega_1 = -0.01$ ,  $\kappa = 1$ ,  $\gamma_M = 0.01$ ,  $\delta_c = -1$  with the same zero initial conditions as Fig.2.

the resonators can freely adjust their relative phases to achieve a synchronized motion [42].

The chaotic dynamics of the mechanical resonator has been found extensively in the conventional optomechanical systems [5–7, 10, 15, 43], but, in a system with both linear and quadratic couplings, the bifurcation and inverse

bifurcation response of the resonator with respect to light driving can be easily modified by the weak quadratic couplings. The sensitive modifications on chaotic transitions in a nearly resolved side-band case ( $\kappa = \omega_M$ ) are shown in Fig.5. The different dynamics under different quadratic couplings clearly verify the parametric modulation effect on the dynamics of the mechanical resonator, which, totally, stabilizes the motion of the resonator (compare Fig.5(a) and Fig.5(c) with Fig.5(b)) [8]. In a weak pumping region, the mechanical resonator damps to the steady states determined by Eq.(5) and Eq.(6) with negative LEs due to energy dissipations and the nonlinear responses in this region can be approximately explained by the dynamics under an adiabatic potential of Eq.(7) [12]. With an increasing pumping power, the damping of the oscillation will be suppressed and a stable SSO is established due to an energy balance [13, 34], which gives zero MLE as shown at the bottom frames of Fig.5. The interesting thing is that the resonator will adjust its position with a process of bifurcation and inverse bifurcation, and then follows by a jumping to a larger position with another bifurcations. The MLE shown in Fig.5 indicates that there exist several bifurcation windows under different pumping powers and one of which is picked to show by the insets in Fig.5. When the pumping light becomes very strong, the mechanical resonator will lock itself to a stable oscillation governed by the strong light pressure of  $-2\omega_1 I(\tau)$ . In this extreme case, the resonator will be approximately treated as a forced resonator because the right term of Eq.(3) will dominate the resonator's dynamics.

## V. FIELD INDICATOR OF THE CHAOTIC TRANSITION

As the intensity of the cavity field parametrically couples to the motion of mechanical resonator, the dynamical transition of the mechanical resonator can influence the cavity field with a back-action effect. By investigating the power spectral density (PSD) of the field emitted from the cavity, we can easily detect and trace the dynamics of the mechanical resonator. Fig.6(a)-(d) present four sample orbits of the mechanical resonator in the phase space, and the corresponding power spectra of the cavity fields are displayed in the right column, (e)-(h), with a negative quadratic coupling rate. Fig.6 indicates a close connection of the mechanical dynamics with the power spectrum of the cavity field intensity  $I_s(t)$ . In a relative low pumping power at  $\eta = 33$ , the resonator maintains its intrinsic frequency on a limit circle but has a very weak backaction on the cavity field. The power spectrum of the cavity field only exhibits a very weak side-band peak near the field-modulated frequency of  $\Omega$  (see Eq.(3)) and a relative stronger peak near  $2\Omega$ . This spectral profile can be understood by the phase trajectory of the field quadratures,  $X$  and  $Y$ , shown by the inset of Fig.6(e). When the pumping amplitude increases

to  $\eta = 34$ , the resonator steps into a period-doubling region and the power spectrum exhibits more resonant side-band peaks at harmonic and subharmonic frequencies around  $\omega_c \pm n\Omega/m$ , where  $n$  and  $m$  are integers. A chaotic dynamics (MLE is positive) of the resonator at pumping amplitude of  $\eta = 40$  will induce a nearly continuous power spectrum as shown in Fig.6(g) [6]. When the pumping amplitude reaches  $\eta = 43$ , the mechanical resonator returns back to a limit-circle dynamics and the corresponding power spectrum displays only sideband peaks as shown in Fig.6(h) [5]. Therefore the power spectrum of the cavity field can be an indicator to trace the dynamical transitions of the mechanical resonator and then a feedback control on the dynamical transition of the mechanical resonator can be developed.

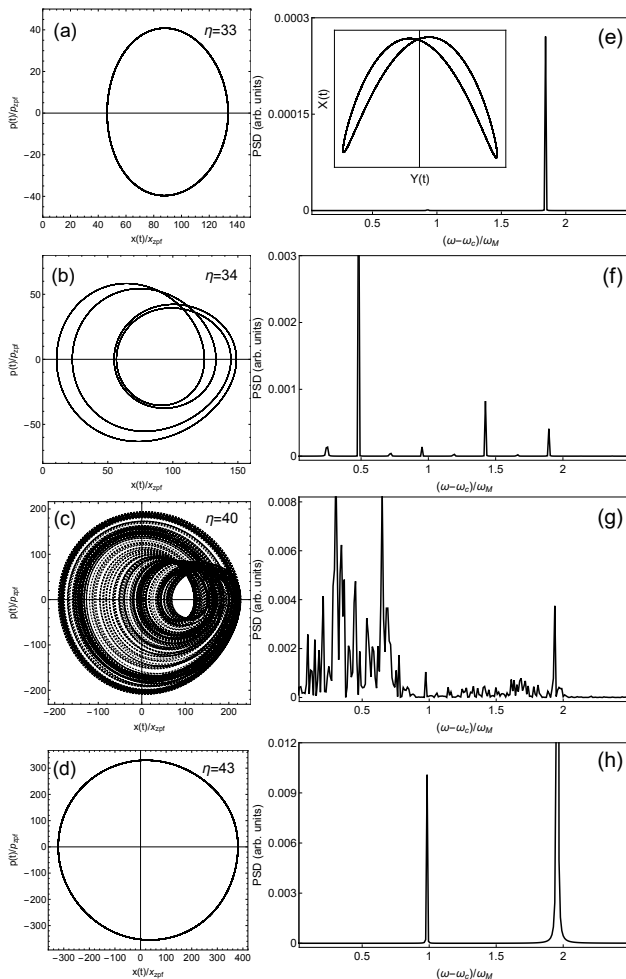


FIG. 6: The dynamical orbits of the mechanical oscillator in the phase space (the left column) and the corresponding power spectral density of the cavity fields (the right column). The dynamical parameters are  $\delta_c = -1$ ,  $\kappa = 1$ ,  $\gamma = 0.01$ ,  $\omega_1 = -0.01$  and  $\omega_2 = -10^{-5}$ .

## VI. CONCLUSIONS AND DISCUSSION

By analyzing an optomechanical system with both linear and quadratic couplings, we find an interesting

chaotic bifurcation and inverse bifurcation of the resonator based on the classical dynamics of Eq.(2) in a red-detuned pumping field. We investigate the parametric effects of the quadratic couplings to modify the dynamics of mechanical resonator and compare the different dynamical transitions between limit-circle oscillations and the chaotic dynamics. The static analysis reveals a very sensitive quadratic effect on the position control of the mechanical resonator. The dynamical calculations give new features of the quadratic couplings and find an interesting dynamical bifurcation of the mechanical resonator inducing different backactions on the field spectrum. Our study, firstly, shows that the optomechanical system with quadratic coupling provide a parametric modification which can be actuated and controlled simultaneously by the intensity of the field. This full optical parametric system has advantages that its nonlinear behavior can be easily controlled by the pumping field and it can work in a red-detuned region with a low thermal noise. The parametric effect found in this system gives a controllable system to study the dynamical transitions, chaotic behaviors and the parametric modulation under a crossover from classical to quantum regime [44]. The study of classical squeezing [23, 31] verified by the parametric effect also presents refined applications based on the nonlinearity of this system, such as to realize coherent frequency mixing and nonlinear-coupled network of optomechanical systems with quadratic couplings. The classical dynamics shows the possibility of squeezing the resonator by quadratic coupling along with a cooling by the linear coupling simultaneously [23]. The dynamics of this system are much more richer than the conventional optomechanical system, and it can be easily detected by the power spectra of the field mode.

With both the quadratic and linear coupling, the quantum chaotic effects near the ground state will be an interesting topic on this model [43]. The quadratic coupling can generate non-classical states and give quantum nondemolition measurement on the energy of the nano-mechanical resonator [45, 46]. In quantum regime, the strong cross-correlation between the light's and the oscillator's motion will lead to new dynamical features above the classical dynamics. To explore these possibilities, a further work of nonlinear effect on quantum dynamics should be done on this model.

## Acknowledgments

This work is supported by the National Science Foundation (Grant No.11447025) and the Scientific Research Foundation for Returned Overseas Chinese Scholars, State Education Ministry.

- [1] M. Aspelmeyer, T. J. Kippenberg, and F. Marquardt, *Cavity optomechanics*, Rev. Mod. Phys. **86**, 1391 (2014).
- [2] A. A. Clerk, M. H. Devoret, S. M. Girvin, F. Marquardt, and R. J. Schoelkopf, *Introduction to quantum noise, measurement, and amplification*, Rev. Mod. Phys. **82**, 1155 (2010).
- [3] M. Poot and H. S. J. vander Zant, *Mechanical systems in the quantum regime*, Phys. Rep. **511**, 273 (2012).
- [4] M. Aspelmeyer, P. Meystre and K. Schwab, *Quantum optomechanics*, Phys. Today **65**, 29 (2012).
- [5] F. Marquardt, G. E. Harris, and S. M. Girvini, *Dynamical Multistability Induced by Radiation Pressure in High-Finesse Micromechanical Optical Cavities*, Phys. Rev. Lett. **96**, 103901 (2006).
- [6] T. Carmon, M. C. Cross, and Kerry J. Vahala, *Chaotic Quivering of Micron-Scaled On-Chip Resonators Excited by Centrifugal Optical Pressure*, Phys. Rev. Lett. **98**, 167203 (2007).
- [7] F. Mueller, S. Heugel, and L. J. Wang, *Observation of optomechanical multistability in a high-Q torsion balance oscillator*, Phys. Rev. A **77**, 031802(R) (2008).
- [8] J. Gieseler, M. Spasenović, L. Novotny and R. Quidant, *Nonlinear Mode Coupling and Synchronization of a Vacuum-Trapped Nanoparticle*, Phys. Rev. Lett. **112**, 103603 (2014).
- [9] C. Metzger, M. Ludwig, C. Neuenhahn, A. Ortlieb, I. Favero, K. Karrai, F. Marquardt, *Self-Induced Oscillations in an Optomechanical System Driven by Bolometric Backaction*, Phys. Rev. Lett. **101**, 133903 (2008).
- [10] T. Carmon, H. Rokhsari, L. Yang, T. J. Kippenberg and K. J. Vahala, *Temporal behavior of radiation-pressure-induced vibrations of an optical microcavity phonon mode*, Phys. Rev. Lett. **94**, 223902 (2005).
- [11] H. Okamoto, D. Ito, K. Onomitsu, H. Sanada, H. Gotoh, T. Sogawa, H. Yamaguchi, *Vibration Amplification, Damping, and Self-Oscillations in Micromechanical Resonators Induced by Optomechanical Coupling through Carrier Excitation*, Phys. Rev. Lett. **106**, 036801 (2011).
- [12] S. Zaitsev, A. K. Pandey, O. Shtempluck, and E. Buks, *Forced and self-excited oscillations of an optomechanical cavity*, Phys. Rev. E **84**, 046605 (2011).
- [13] L. Zhang and H. Kong, *Self-sustained oscillation and harmonic generation in optomechanical systems with quadratic couplings*, Phys. Rev. A **89**, 023847 (2014).
- [14] A. Jenkins, *Self-oscillation*, Phys. Rep. **525**, 167 (2013).
- [15] L. Bakemeier, A. Alvermann, and H. Fehske, *Route to Chaos in Optomechanics*, Phys. Rev. Lett. **114**, 013601 (2015).
- [16] J. D. Thompson, B. M. Zwickl, A. M. Jayich, F. Marquardt, S. M. Girvin and J. G. E. Harris, *Strong dispersive coupling of a high-finesse cavity to a micromechanical membrane*, Nature **452**, 72 (2008).
- [17] D. E. Chang, C. A. Regal, S. B. Papp, D. J. Wilson, J. Ye, O. Painter, H. J. Kimble and P. Zoller, *Cavity optomechanics using an optically levitated nanosphere*, PNAS **107**, 1005 (2010).
- [18] J. C. Sankey, C. Yang, B. M. Zwickl, A. M. Jayich and J. G. E. Harris, *Strong and tunable nonlinear optomechanical coupling in a low-loss system*, Nature Physics **6**, 707 (2010).
- [19] V. Peano and M. Thorwart, *Macroscopic quantum effects in a strongly driven nanomechanical resonator*, Phys. Rev. B **70**, 235401 (2004).
- [20] H. G. Craighead, *Nanoelectromechanical Systems*, Science **290**, 1532 (2000).
- [21] T. P. Purdy, D. W. C. Brooks, T. Botter, N. Brahms, Z.-Y. Ma and D. M. Stamper-Kurn, *Tunable Cavity Optomechanics with Ultracold Atoms*, Phys. Rev. Lett. **105**, 133602 (2010).
- [22] S. Gupta, K. L. Moore, K. W. Murch and D. M. Stamper-Kurn, *Cavity Nonlinear Optics at Low Photon Numbers from Collective Atomic Motion*, Phys. Rev. Lett. **99**, 213601 (2007).
- [23] A. Nunnenkamp, K. Børkje, J. G. E. Harris and S. M. Girvin, *Cooling and squeezing via quadratic optomechanical coupling*, Phys. Rev. A **82**, 021806(R) (2010).
- [24] S. Gröblacher, K. Hammerer, M. R. Vanner, and M. Aspelmeyer, *Observation of strong coupling between a micromechanical resonator and an optical cavity field*, Nature **460**, 724 (2009).
- [25] O. Arcizet, P. -F. Cohadon, T. Briant, M. Pinard and A. Heidmann, *Radiation-pressure cooling and optomechanical instability of a micromirror*, Nature **444** 71 (2006).
- [26] J. S. Aldridge and A. N. Cleland, *Noise-Enabled Precision Measurements of a Duffing Nanomechanical Resonator*, Phys. Rev. Lett. **94**, 156403 (2005).
- [27] I. Katz, A. Retzker, R. Straub, and R. Lifshitz, *Signatures for a Classical to Quantum Transition of a Driven Nonlinear Nanomechanical Resonator*, Phys. Rev. Lett. **99**, 040404 (2007).
- [28] Warner J. Venstra<sup>1</sup>, Hidde J. R. Westra, Herre S.J. van der Zant, *Stochastic switching of cantilever motion*, Nat. Comm. **4**, 2624 (2013).
- [29] I. Favero and K. Karrai, *Optomechanics of deformable optical cavities*, Nature Photonics **3**, 201 (2009).
- [30] J. Chan, A. H. Safavi-Naeini, J. T. Hill, S. Meenehan and O. Painter, *Optimized optomechanical crystal cavity with acoustic radiation shield*, Appl. Phys. Lett. **101**, 081115 (2012).
- [31] D. Rugar, P. Grütter, *Mechanical parametric amplification and thermomechanical noise squeezing*, Phys. Rev. Lett. **67**, 699 (1991).
- [32] K. L. Turner, S. A. Miller, P. G. Hartwell, N. C. MacDonald, S. H. Strogatz, S. G. Adams, *Five parametric resonances in a micromechanical system*, Nature **396**, 149 (1998).
- [33] Junho Suh, M. D. LaHaye, P. M. Echternach, K. C. Schwab and M. L. Roukes, *Parametric Amplification and Back-Action Noise Squeezing by a Qubit-Coupled Nanoresonator* Nano Lett. **10**, 3990 (2010).
- [34] M. Ludwig, B. Kubala and F. Marquardt, *The optomechanical instability in the quantum regime*, New J. Phys. **10**, 095013 (2008).
- [35] L. Zhang and Z. Song, *Modification on static responses of a nano-oscillator by quadratic opto-mechanical couplings*, Sci. China Phys. Mech. Astron. **57**, 880 (2014).
- [36] I. Kozinsky, H. W. Ch. Postma, O. Kogan, A. Husain, and M.L. Roukes, *Basins of Attraction of a Nonlinear Nanomechanical Resonator*, Phys. Rev. Lett. **99**, 207201 (2007).
- [37] A. Dorsel, J. D. McCullen, P. Meystre, E. Vignes, and H. Walther, *Optical Bistability and Mirror Confinement*

- Induced by Radiation Pressure*, Phys. Rev. Lett. **51**, 1550 (1983).
- [38] J. S. W. Lamb, and J. A. G. Roberts, *Time-reversal symmetry in dynamical systems: A survey*, Physica D **112**, 1 (1998).
- [39] G. Heinrich, M. Ludwig, J. Qian, B. Kubala, and F. Marquardt, *Collective Dynamics in Optomechanical Arrays*, Phys. Rev. Lett. **107**, 043603 (2011).
- [40] M. Hossein-Zadeh and K. J. Vahala, *Observation of optical spring effect in a microtoroidal optomechanical resonator*, Opt. Lett. **32**, 1611 (2007).
- [41] B. S. Sheard, M. B. Gray, C. M. Mow-Lowry, D. E. McClelland and S. E. Whitcomb, *Observation and characterization of an optical spring*, Phys. Rev. A **69**, 051801(R) (2004).
- [42] A. Pikovsky, M. Rosenblum and J. Kurths, *Synchronization: a universal concept in nonlinear sciences*, Cambridge University Press, Cambridge UK (2001).
- [43] X. Lü, H. Jing, J. Ma, and Y. Wu, *PT-Symmetry-Breaking Chaos in Optomechanics*, Phys. Re. Lett. **114**, 253601 (2015).
- [44] R. B. Karabalin, X. L. Feng, and M. L. Roukes, *Parametric Nanomechanical Amplification at Very High Frequency*, Nano Lett. **9**, 3116 (2009).
- [45] J. Milburn, D. F. Walls, *Quantum nondemolition measurements via quadratic coupling*, Phys Rev A **28**, 2065 (1983).
- [46] M. R. Vanner, *Selective Linear or Quadratic Optomechanical Coupling via Measurement*, Phys. Re. X **1**, 021011 (2011).